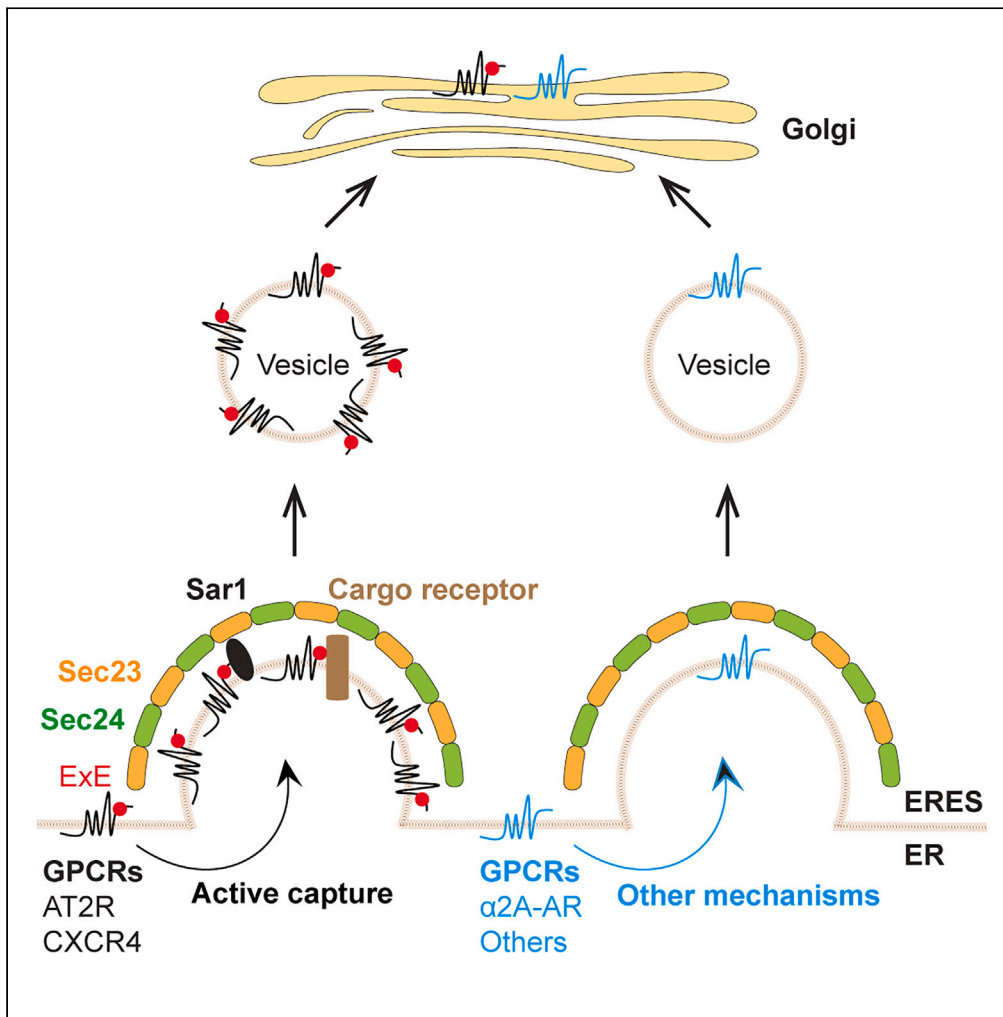


Article

# Sequence-directed concentration of G protein-coupled receptors in COPII vesicles



Xin Xu, Nevin A. Lambert, Guangyu Wu

guwu@augusta.edu

**Highlights**  
Some GPCRs are highly concentrated at ERES

AT2R and CXCR4 recruitment to ERES are mediated via distinct motifs

AT2R interacts with Sar1 GTPase

Distinct GPCRs have different ER export kinetics via COPII vesicles

Xu et al., iScience 26, 107969  
October 20, 2023 © 2023 The Author(s).  
<https://doi.org/10.1016/j.isci.2023.107969>

## Article

## Sequence-directed concentration of G protein-coupled receptors in COPII vesicles

Xin Xu,<sup>1</sup> Nevin A. Lambert,<sup>1</sup> and Guangyu Wu<sup>1,2,\*</sup>

## SUMMARY

**G protein-coupled receptors (GPCRs) constitute the largest superfamily of plasma membrane signaling proteins. However, virtually nothing is known about their recruitment to COPII vesicles for forward delivery after synthesis in the endoplasmic reticulum (ER). Here, we demonstrate that some GPCRs are highly concentrated at ER exit sites (ERES) before COPII budding. Angiotensin II type 2 receptor (AT2R) and CXCR4 concentration are directed by a di-acidic motif and a 9-residue domain, respectively, and these motifs also control receptor ER-Golgi traffic. We further show that AT2R interacts with Sar1 GTPase and that distinct GPCRs have different ER-Golgi transport rates via COPII which is independent of their concentration at ERES. Collectively, these data demonstrate that GPCRs can be actively captured by COPII via specific motifs and direct interaction with COPII components that in turn affects their export dynamics, and provide important insights into COPII targeting and forward trafficking of nascent GPCRs.**

## INTRODUCTION

With more than 800 members, G protein-coupled receptors (GPCRs) constitute the largest and most structurally diverse superfamily of plasma membrane (PM) signaling proteins; they regulate a wide range of physiological and pathological processes and are actual therapeutic targets of human diseases.<sup>1,2</sup> All GPCRs share similar structural features with seven transmembrane  $\alpha$ -helical domains connected with three intracellular loops and three extracellular loops. The extracellular part of the receptor binds to specific ligands, such as hormones, neurotransmitters, or drugs, which activate the receptor and trigger signal transduction pathways, while the intracellular part of the receptor activates downstream signaling molecules, such as G proteins and arrestins,<sup>3–5</sup> and interacts with regulatory proteins involved in receptor trafficking, phosphorylation, and signaling initiation and termination.<sup>6–9</sup>

The endoplasmic reticulum (ER) is a network of membranous tubules and flattened cisternae where, similar to many other PM proteins, GPCRs are synthesized and undergo a complex process of folding, maturation, modification, and assembly before they are exported and delivered to the cell surface. As compared with the well-characterized internalization process in which GPCRs at the cell surface are transported to endosomes after agonist stimulation, the molecular mechanisms underlying anterograde transport of GPCRs are relatively much less well understood. Emerging evidence from the studies in the past 3 decades suggests that GPCR transport from the ER to the cell surface is a sophisticated, dynamic process which is regulated by many factors, including structural determinants embedded within the receptors<sup>10,11</sup> and various regulatory proteins.<sup>12–27</sup>

Coat protein complex II (COPII) vesicles exclusively mediate the export of newly synthesized cargoes from the ER to the ER-Golgi intermediate complex (ERGIC). The first step in the formation of COPII vesicles is the activation of the small GTPase Sar1 on the ER exit sites (ERES) by the transmembrane guanine nucleotide exchange factor Sec12. Once activated, Sar1 inserts its hydrophobic N terminus into the ER membrane and membrane-bound Sar1 then interacts with Sec23 to recruit heterodimeric Sec23-Sec24 complex, the inner layer of COPII vesicles, to the ERES. The Sec23-Sec24 complex subsequently recruits the Sec13-Sec31 complex, the outer layer of COPII vesicles, forming a lattice or cage-like structure. This lattice deforms the ER membrane, leading to the formation of a bud that eventually pinches off to form a COPII vesicle.<sup>28–30</sup> The peripheral protein Sec16 acts as a scaffold to associate with multiple components of COPII vesicles, stabilize COPII components on the ER membrane, and enhance the formation of ERES and COPII vesicles. More recent studies have revealed a COPII-regulated tubular network for ER-Golgi protein transport<sup>31</sup> and also demonstrated that COPII coat proteins function as a gatekeeper at the boundary between the ER and the ERES in selecting and concentrating cargo molecules and remain associated with the ER membrane at the ERES during cargo export.<sup>32,33</sup>

In order to be efficiently exported in COPII vesicles, some cargo proteins interact with Sec24 isoforms via ER export motifs, which are short, linear sequences presented in the C termini of the cargoes, or ER-localized transmembrane proteins referred to as cargo receptors which interact with Sec24.<sup>34–41</sup> Structural studies have revealed multiple, distinct cargo-binding sites on Sec24 which allows for efficient

<sup>1</sup>Department of Pharmacology and Toxicology, Medical College of Georgia, Augusta University, Augusta, GA 30912, USA

<sup>2</sup>Lead contact

\*Correspondence: [guwu@augusta.edu](mailto:guwu@augusta.edu)  
<https://doi.org/10.1016/j.isci.2023.107969>



accommodation of diverse cargo molecules.<sup>42</sup> Of various ER export motifs identified, the di-acidic motifs (E/DxD/E) are the best studied, and well-characterized examples have been found in the cytoplasmic C termini of several membrane proteins.<sup>38,43–46</sup>

Despite some evidence suggesting the possible roles for COPII vesicles in the ER export of some GPCRs,<sup>16,47–50</sup> there remains no direct evidence indicating that nascent GPCRs are actively recruited to and concentrated in COPII vesicles. Although several motifs or sequences have been shown to be important for GPCR export from the ER,<sup>50–61</sup> none of them have been proven to directly act on receptor recruitment to COPII vesicles. Here, we have demonstrated that angiotensin II (Ang II) receptors and the chemokine receptor CXCR4 are concentrated at the ERES and COPII vesicles through distinct motifs and this concentrative process affects receptor anterograde transport from the ER through the Golgi to the PM. These data reveal for the first time that ER export of some GPCR members is an active process, involving specific motifs for selective capture by COPII vesicles on the ER membrane.

## RESULTS

### Screening for GPCRs that are concentrated in COPII vesicles

As an initial approach to search for GPCRs that are actively recruited to COPII vesicles, we used the retention using the selective hooks (RUSH) assays<sup>27,62</sup> to screen a group of family A GPCRs, including Ang II type 1 and type 2 receptors (AT1R and AT2R), chemokine receptor CXCR4, adrenergic receptors ( $\alpha_{2A}$ -AR,  $\alpha_{2B}$ -AR, and  $\beta_2$ -AR), dopamine D2 receptor (D2R), muscarinic acetylcholine receptor type 3 (M3R), adenosine A2A receptor (A2AR),  $\delta$  opioid receptor (DOR), 5-hydroxytryptamine receptor 1B (5HT1BR), and vasopressin V2 receptor (V2R). In RUSH assays, individual GPCRs are conjugated with GFP and a streptavidin-binding peptide (SBP), and the ER retention signal KDEL fused to streptavidin is used as a hook (Figure 1A). The ER export of the receptors is synchronized after addition of biotin to disrupt SBP-streptavidin interaction. As vesicular stomatitis virus glycoprotein (VSVG) has been well described to concentrate in COPII vesicles via direct interaction with Sec24 using the di-acidic motif DxE in the C terminus,<sup>35–41</sup> it was used as a positive control. Indeed, a large number of punctate structures containing VSVG were visualized in both HeLa and HEK293 cells without incubation with biotin to induce ER export (Figure 1B).

Among the 12 GPCRs studied, AT2R, CXCR4, and AT1R were found to clearly concentrate in puncta in the absence of biotin (Figure 1C). The numbers of puncta in cells expressing individual cargoes were in the order of VSVG>AT2R>CXCR4>AT1R (Figure 1D). In contrast, very few or no punctate structures were detected in cells expressing  $\alpha_{2A}$ -AR,  $\alpha_{2B}$ -AR,  $\beta_2$ -AR, D2R, M3R, A2AR, DOR, 5HT1BR, or V2R (Figure 1E). Similar results were obtained in HeLa and HEK293 cells, albeit the numbers of puncta in HeLa cells were relatively higher than those in HEK293 cells (Figures 1B–1E). As the number of puncta in cells expressing AT1R was relatively low, the formation of puncta containing this receptor was not studied further.

To confirm that the puncta observed were indeed the ERES, we used Sec24D as a marker of the ERES and determined the effect of inhibiting Sar1 function via expression of GTP-bound Sar1H79G mutant on the formation of puncta. Sec24D was strongly co-localized with VSVG (Figure 2A), AT2R (Figure 2B), and CXCR4 (Figure 2C) in puncta. Expression of Sar1H79G abolished the formation of punctate structures in cells expressing VSVG, AT2R, or CXCR4 (Figure S1). These data demonstrate that, similar to VSVG, some, but not all, GPCR members are actively recruited to and highly concentrated at the ERES before COPII vesicle budding from the ER membrane.

### AT2R and CXCR4 use different motifs for recruitment to ERES

To define specific motifs that mediate AT2R and CXCR4 recruitment to the ERES and COPII vesicles, we focused on the di-acidic motif ExE in the membrane-distal, nonstructural portions of the C termini, similar to the location of the DxE motif in VSVG (Figure 2D). As expected, mutation of DxE to AxA markedly disrupted VSVG recruitment to the ERES using Sec24D as a marker (Figure 2E). Similarly, mutation of the motif ExE to AxA disrupted AT2R co-localization with Sec24D, indicative of ineffective targeting to the ERES (Figure 2F). However, the CXCR4 mutant in which the motif ExE was mutated to AxA was transported normally to the ERES (Figure 2G). As basic motifs also play a role in cargo export from the ER,<sup>50,63,64</sup> we measured the effect of mutating three basic residues in the C-terminal sequence KGKR on CXCR4 concentration at the ERES. Mutation of KGKR to AGAA also did not alter CXCR4 targeting to the ERES (Figure 2H). Quantitative data further showed that mutation of the di-acidic motifs markedly inhibited VSVG and AT2R recruitment to the punctate structures (Figure 2I) and their co-localization with Sec24D in the whole cell (Figure 2J) and at the ERES (Figure 2K), whereas mutating the acidic and basic motifs did not affect CXCR4 recruitment and co-localization with Sec24D. These data indicate that AT2R, but not CXCR4, uses the C-terminal ExE motif for its targeting to the ERES.

We next used a progressive deletion strategy to identify specific sequences responsible for CXCR4 recruitment to the ERES (Figure 3A). Deletion of the whole C terminus or the last 39 amino acid residues clearly disrupted CXCR4 localization to the ERES, whereas deletion of the last 30 residues had no apparent effect on CXCR4 transport to the ERES, in RUSH assays in both HeLa (Figures 3B and 3D) and HEK293 cells (Figures 3C and 3D). These data suggest that the C-terminal fragment QHALTSVSR likely directs CXCR4 capture and concentration at the ERES.

### ERES concentration controls the ER-to-Golgi export kinetics of AT2R and CXCR4

We then determined the role of COPII concentration in the export of AT2R and CXCR4 in both live and fixed cell RUSH assays. We first compared the ER-to-Golgi transport kinetics of VSVG and AT2R with their mutants lacking the di-acidic motifs by quantifying their Golgi expression in live cell RUSH assays. AT2R transport to the Golgi compartments via the ERGIC after biotin induction was confirmed by co-localization with the ERGIC marker p58 (Figure S2A) and the Golgi markers giantin (a *cis*- and *medial*-Golgi marker) (Figure S2B)

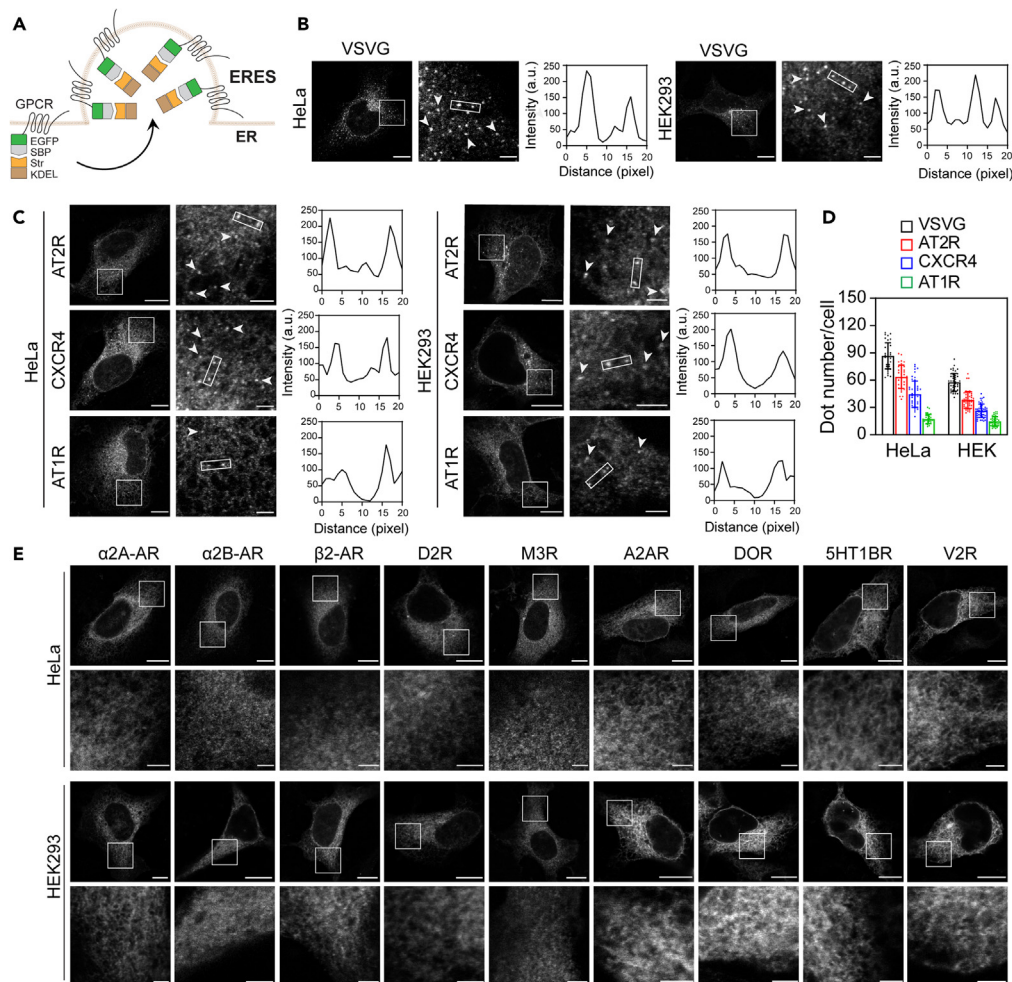


**Figure 1. Screening for GPCRs that are concentrated at the ERES in RUSH assays**

(A) Cartoon of the RUSH system for the expression and recruitment of GPCRs at the ERES. (B) Representative images showing VSVG concentration in puncta in HeLa and HEK293 cells. (C) Concentration of AT2R, CXCR4, and AT1R in puncta in HeLa and HEK293 cells. (D) Quantification of puncta in cells expressing VSVG and GPCRs. The quantitative data are the number of puncta per cell and expressed as mean  $\pm$  SD ( $n = 30$ – $50$  cells in at least 5 separate experiments). (E) Representative images showing GPCRs that barely form puncta in HeLa and HEK293 cells. In (B), (C), and (E), GPCRs or VSVG in RUSH plasmids were expressed in cells and their localization were visualized by confocal imaging without addition of biotin. Arrows indicate cargo-containing punctate structures. Magnification of boxed areas is shown on the right (B and C) or below (E). The quantitative data shown in (B) and (C) are the cargo intensities in rectangle boxes. Scale bars, 10 and 2.5  $\mu$ m (insets).

and  $\beta$ 1,4-galactosyltransferase 1 (a *trans*-Golgi and *trans*-Golgi network marker) (Figures S2C and S2D). After addition of biotin for about 10 min, VSVG was already transported to the Golgi and the strongest VSVG expression was observed at 20 to 30 min. At about 45 min, VSVG expression at the Golgi begun to decline, indicative of post-Golgi transport (Figures 4A and 4B). AT2R was clearly seen at the Golgi at about 15 min and its strongest Golgi expression was observed after 30 min of biotin incubation. The majority of AT2R remained at the Golgi after biotin induction for 60 min (Figures 4C and 4D). These data suggest that both the ER-Golgi and Golgi-PM transport of AT2R are slightly slower than VSVG transport. Mutation of the DxE motif in VSVG and mutation of the ExE motif in AT2R markedly impeded their export to the Golgi and the time-course curves of CXCR4 and AT2R mutants were apparently delayed (Figure 4). Mutated VSVG and AT2R were not obviously transported to the Golgi until biotin incubation for 30 and 40 min, respectively (Figures 4A and 4C; Videos S1 and S2). The maximal Golgi expression was attenuated by approximately 50% in cells expressing mutated VSVG and AT2R as compared with their wild-type counterparts (Figures 4B and 4D).

In fixed cell RUSH assays, VSVG transport was measured at 10 and 20 min after biotin incubation, whereas AT2R and CXCR4 transport were measured at 15 and 30 min. Similar to the results obtained in live cells, the Golgi expression of mutated VSVG and AT2R at both time points was significantly lower than those of their wild-type counterparts (Figures 5A–5C). For CXCR4, deletion of the last 39 residues (1–313)

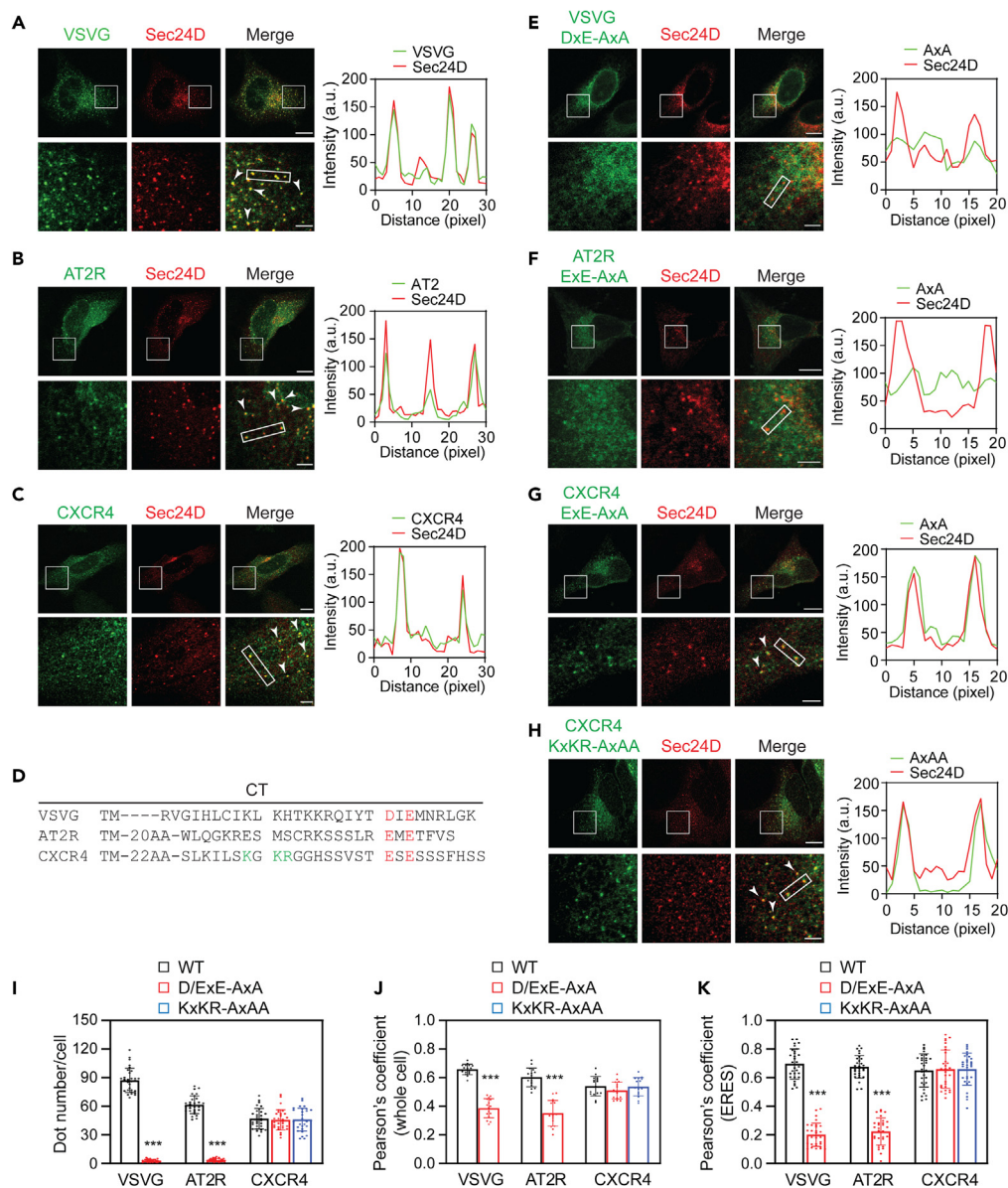


**Figure 2. GPCR recruitment to the ERES and effects of mutating the acidic and basic motifs**

(A–C) Co-localization of VSVG (A), AT2R (B), and CXCR4 (C) with Sec24D in HeLa cells.

(D) Alignment of the di-acidic motifs in the membrane-distal C termini. TM, transmembrane domain; CT, C terminus.

(E–G) Effects of mutating the di-acidic motifs on the concentration of VSVG (E), AT2R (F), and CXCR4 (G) at the ERES using Sec24D as a marker in HeLa cells.

(H) Effect of mutating KxKR to AxAA on CXCR4 expression at the ERES. The cells were transfected with individual GFP-tagged cargoes or their mutants together with DsRed-tagged Sec24D. Arrows indicate co-localization of cargoes with Sec24D at the ERES. Similar results were obtained in 3–5 repeats. Scale bars, 10 and 2.5  $\mu$ m (insets).

(I) Quantification of the punctate structures containing individual cargoes and their mutants. The quantitative data are the number of puncta per cell and expressed as mean  $\pm$  SD ( $n = 30$  cells in 3 separate experiments).

(J and K) Quantification of Pearson's coefficient between individual cargoes and Sec24D in the whole cell (J) and in the punctate structures (K). The quantitative data are expressed as mean  $\pm$  SD ( $n = 16$  cells from 3 experiments in J and  $n = 30$  vesicles in 10 cells from 3 experiments in K). \*\*\* $p < 0.001$  vs. respective WT counterparts.

significantly reduced the Golgi expression, whereas the deletion mutant lacking the last 30 residues (1–322) was delivered normally to the Golgi (Figures 5D and 5E).

To address the question of whether GPCR concentration in COPII could affect their transport to the cell surface where is the functional destination for most GPCRs, we used the HiBit protein tagging system to insert HiBit (11 amino acid peptide) between EGFP and SBP in

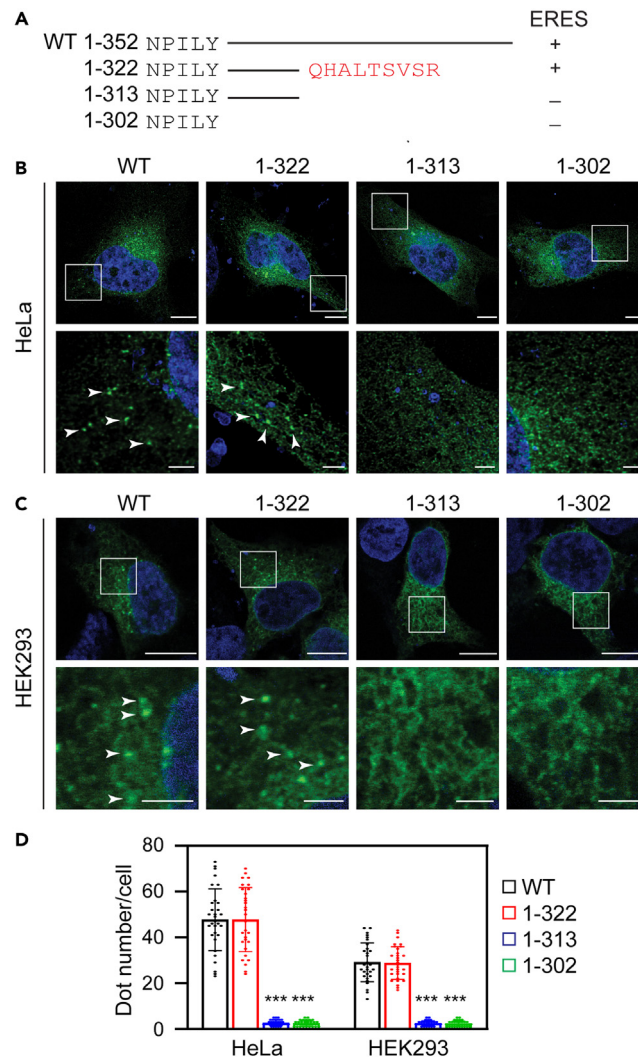


**Figure 3. Identification of specific domains responsible for CXCR4 recruitment to the ERES**

(A) Summary of progressive deletion to identify the sequence QHALTSVSR for CXCR4 inclusion to the ERES. WT, wild type.

(B and C) Representative images showing ERES formation in cells expressing CXCR4 or its deletion mutants in HeLa (B) and HEK293 cells (C). Arrows indicate CXCR4-containing ERES. Similar results were obtained in 3 repeats. Scale bars, 10 and 2.5  $\mu$ m (insets).

(D) Quantification of the punctate structures containing CXCR4 or its truncated mutants. The quantitative data are the number of puncta per cell and expressed as mean  $\pm$  SD (n = 30–35 cells in 3 separate experiments).

the RUSH plasmids of AT2R and its ExE-AxA mutant (Figure 5F). After the cells were transfected with the plasmids and incubated with biotin for 60 min, receptor expression at the cell surface was quantified by measuring the luminescence signal after addition of LgBiT (Figure 5F). The surface expression of mutated AT2R carrying ExE-AxA mutation was reduced by approximately 50% as compared with wild-type AT2R (Figure 5G). These data demonstrate that the ExE motif controls not only AT2R recruitment to COPII vesicles but also its export from the ER to the Golgi and the cell surface.

### AT2R interacts with Sar1 GTPase

To explore the mechanisms underlying the function of the ExE motif in AT2R recruitment to COPII vesicles, we determined if the ExE motif could mediate AT2R interaction with COPII components, including Sec24 A/B/C/D, Sec23 A/B, Sec16, and Sar1 in GST fusion protein pull-down and co-immunoprecipitation (co-IP) assays. GST fusion proteins containing the C terminus of AT2R (AT2Rct) interacted with both GFP-tagged Sar1 (Figure 6A) and Myc-tagged Sar1 (Figure 6B). However, mutation of the ExE motif did not influence AT2Rct interaction with Sar1 (Figures 6A and 6B). In contrast, both AT1Rct and its ExE-AxA mutant did not interact with GFP-tagged Sec24, Sec23, and Sec16 in GST fusion protein pull-down assays (Figure 6A). Similarly, in co-IP assays, full-length AT2R formed a complex with Sar1, but not with Sec24 isoforms, and

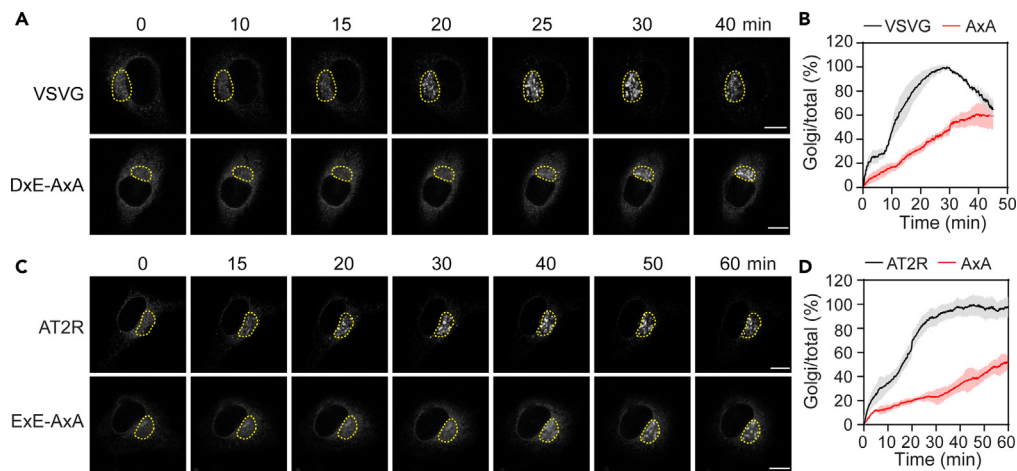


**Figure 4. Mutation of the di-acidic motifs inhibits the ER-Golgi export kinetics of VSVG and AT2R in live cell RUSH assays**

(A) Representative images showing ER-Golgi export of VSVG and its DxE-AxA mutant over time in RUSH assays in live cells.

(B) Quantitative data shown in (A).

(C) Representative images showing ER-Golgi export of AT2R and its ExE-AxA mutant in live cells.

(D) Quantitative data shown in (C). HeLa cells were transfected with RUSH plasmids for 20 h and the ER export was induced by addition of biotin at 0 min. The Golgi expression of individual cargoes after biotin incubation for different time periods was measured by the fluorescence intensity in the area containing highly concentrated cargoes (yellow lines) using ImageJ. The quantitative data are expressed as the ratio of the Golgi expression to the total expression. The Golgi/total ratio at each time point was subtracted from the ratio at time 0 and then normalized to the ratio of wild-type cargoes. The data shown are mean  $\pm$  SD (n = 5–8 cells in 3 experiments). Scale bars, 10  $\mu$ m.

mutation of the ExE motif did not affect AT2R interaction with Sar1 (Figure 6C). These data suggest that AT2R directly interacts with Sar1 GTPase and the interaction is independent of the ExE motif.

### Comparison of the ER-Golgi transport of different GPCR members via COPII vesicles

We next sought to compare the ER-Golgi transport rates of different GPCRs by measuring their Golgi expression at 15 and 30 min after biotin incubation in fixed cell RUSH assays. We found that the ER-Golgi transport of 6 GPCRs, including AT2R, CXCR4,  $\alpha_{2A}$ -AR,  $\alpha_{2B}$ -AR,  $\beta_2$ -AR, and D2R, was largely comparable, whereas the ER-Golgi export of AT1R, DOR, 5HT1BR, and V2R was relatively slower (Figures 7A and 7B). These data suggest that distinct GPCRs have different ER-Golgi transport rates. Furthermore, expression of Sar1H79G almost abolished the ER-Golgi transport of all 10 GPCRs studied (Figures 7B and S3). These data demonstrate that COPII vesicles effectively mediate ER-Golgi export of distinct GPCR members, regardless of their concentration at the ERES and in COPII vesicles.

## DISCUSSION

The most important finding presented in this report is that some, but not all, GPCR members are actively recruited to and highly concentrated in COPII vesicles that are directed by specific motifs or sequences and this selective COPII-loading process controls the ER-Golgi export kinetics of the receptors. In particular, we have identified three GPCRs, AT2R, CXCR4, and AT1R, that are concentrated at ERES before COPII vesicle budding from the ER, which was confirmed by using Sec24 as a marker and Sar1 inhibition to block the ERES formation, in RUSH assays. These data suggest that the nascent cargo GPCRs via the RUSH system are correctly folded and properly assembled before biotin addition to release streptavidin-SBP interaction and already packaged into the ERES, competent for export from the ER via COPII vesicles. These three receptors represent the first group of GPCRs that are selectively captured by COPII vesicles (Figure 8A). In contrast, 9 GPCRs, out of 12 studied, are not evident in selective COPII concentration, suggesting that most GPCRs are recruited to COPII vesicles by other mechanisms, such as the default bulk flow in which nascent cargoes passively leave from the ER<sup>65,66</sup> (Figure 8B). It is worth noting that these 9 GPCRs include  $\alpha_{2B}$ -AR that interacts with Sec24C/D via the RRR motif in the third intracellular loop,<sup>50</sup>  $\beta_2$ -AR that interacts with Sec23 and Sec24 via the human cornichon homolog 4 which was proposed to function as a cargo receptor for some GPCRs,<sup>16</sup> and 5HT1BR that was shown to be recruited to secretory vesicles for post-synaptic transport in neurons.<sup>67</sup>

Multiple ER export motifs have been described to dictate COPII recruitment of cargo molecules, including VSVG, cystic fibrosis transmembrane conductance regulator, and potassium channels.<sup>38,43–46</sup> Here, we have demonstrated that selective capture of AT2R and CXCR4 by COPII vesicles is mediated through distinct motifs in the C termini. In particular, the ExE motif directs AT2R concentration at the ERES and COPII vesicles which is consistent with the role of this motif in AT2R export from the ER.<sup>51</sup> Interestingly, the ExE motif in the similar location does not play a major role in CXCR4 loading to COPII vesicles. Instead, we have identified a 9-amino acid domain, QHALTSVSR, in the middle portion of nonstructural C terminus,<sup>68</sup> likely responsible for selective targeting of CXCR4 to COPII vesicles, and this domain is likely unique for CXCR4.

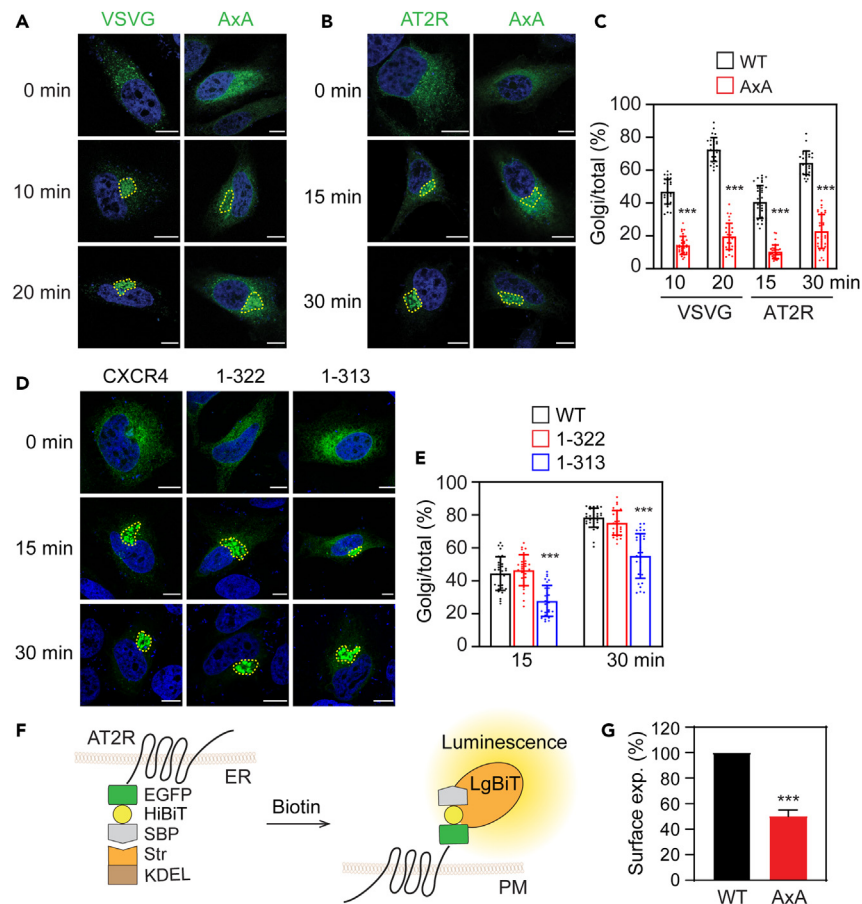


**Figure 5. Mutation or deletion of the motifs responsible for ERES concentration impedes the ER-Golgi transport of AT2R and CXCR4**

(A, B, and D) Representative images showing ER-Golgi transport of VSVG (A), AT2R (B), and CXCR4 (D) in RUSH assays in fixed cells. HeLa cells were transfected with RUSH plasmids for 20 h and fixed at 15 and 30 min after addition of biotin. The Golgi expression of individual cargoes after biotin incubation was measured by the fluorescence intensity in the area containing highly concentrated cargoes (yellow lines).

(C) Quantitative data shown in (A) and (B).

(E) Quantitative data shown in (D). The highly concentrated cargo molecules in the perinuclear region were measured as their expression at the Golgi. The quantitative data are expressed as the ratio of the Golgi expression to the total expression.

(F) Cartoon of the modified RUSH system for measurement of the cell surface expression of AT2R.

(G) Effect of mutating the ExE motif on the cell surface expression of AT2R. HEK293 cells were transfected with RUSH plasmids for 20 h and then incubated with biotin for 1 h. The surface expression of AT2R was quantified by measuring the luminescence signal after addition of LgBiT and substrate. The quantitative data shown are mean  $\pm$  SD ( $n = 30$ – $36$  cells in at least 3 individual experiments in C and E;  $n = 3$  in G). WT, wild type. \*\*\* $p < 0.001$  vs. respective WT counterparts. Scale bars, 10  $\mu$ m.

It is well known that the function of ER export motifs in cargo recruitment to COPII vesicles is mediated through direct interaction with Sec24.<sup>35–41</sup> Here, we found that only Sar1 GTPase, but not other COPII components, binds AT2R, and Sar1 interaction with AT2R is independent of the ExE motif in the receptor. These data suggest that the function of the motif ExE in directing AT2R recruitment to COPII is unlikely mediated through interaction with COPII components. These data also imply two possible mechanisms for AT2R recruitment to COPII vesicles. One is that AT2R interacts with Sar1 to facilitate its concentration in COPII vesicles (Figure 8A). Indeed, Sar1 has been shown to interact with glycosyltransferases to regulate their ER export via COPII vesicles.<sup>63</sup> The other is that AT2R uses the motif ExE to interact with yet unidentified cargo receptors or other regulatory proteins involved in AT2R recruitment to COPII vesicles (Figure 8A). This possibility is supported by the facts that a number of regulatory proteins have been identified to enhance GPCR biosynthetic export<sup>10,11</sup> and AT2R-interacting protein 1 (also known as ATBP50) regulates AT2R transport from the Golgi to the PM.<sup>69</sup>

There are several interesting points regarding the role of selective COPII concentration in GPCR biosynthetic forward trafficking. First, we have demonstrated that mutation of the ExE motif markedly decelerates the ER-Golgi export of AT2R and diminishes its maximal transport to the Golgi and cell surface. Similarly, deletion of the domain QHALTSVSR impedes CXCR4 export from the ER to the Golgi. However, whether or not this domain affects CXCR4 transport to the cell surface is unknown. These data indicate that motif-directed concentration of nascent GPCRs at the ERES and COPII vesicles controls the ER-Golgi export kinetics of the receptors. Second, different GPCRs may have different

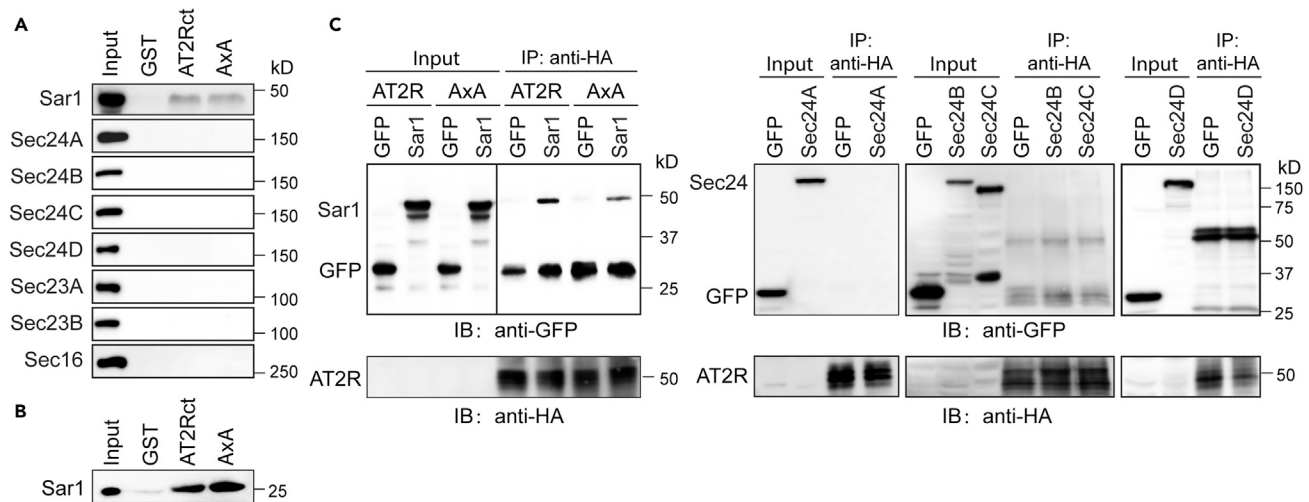


**Figure 6. AT2R interaction with COPII components**

(A) Interaction of AT2Rct and its mutant ExE-AxA with GFP-tagged Sar1, Sec24 A/B/C/D, Sec23 A/B, and Sec16 in GST fusion protein pull-down assays.

(B) Interaction of AT2Rct and its mutant ExE-AxA with Myc-tagged Sar1 in GST fusion protein pull-down assays.

(C) Interaction of full-length AT2R and its mutant ExE-AxA with GFP-tagged Sar1 and Sec24 in co-IP assays. HEK293 cells were transfected with HA-AT2R or its mutant together with GFP (as control), GFP-Sar1, or GFP-Sec24 and subjected to IP with mouse HA antibodies. In immunoblotting, rabbit GFP antibodies were used in Sar1 and Sec24 A/B/C co-IP experiments, whereas mouse GFP antibodies were used in Sec24D co-IP and Ig was detected. In each panel, similar results were obtained in at least 3 replicates. Input contains 3% of the total proteins used in the experiments.

ER-Golgi transport kinetics and expression of SarH79G almost abolishes all GPCR transport. These data suggest that COPII-mediated ER export is sufficient for distinct GPCR members, regardless of whether they are concentrated in COPII vesicles. These data also imply that motif-direct selective capture and bulk flow mechanism for GPCR recruitment to COPII vesicles are equally important for effectively delivering the receptors from the ER to the Golgi. Third, it is apparent that the abilities of GPCRs for concentration in the ERES and COPII vesicles are largely variable and all of them as studied here are less than VSVG. As such, it is quite possible that most GPCRs utilize both selective capture and bulk flow mechanisms for their COPII recruitment and the dominant mechanism utilized by individual receptors may be determined by the nature of specific structure and functional requirement of the receptors. It should be pointed out that although GPCRs in family A were investigated here, the conclusions of the study can be applied to other GPCR families.

It is becoming increasingly clear that nascent GPCR export from the ER represents a crucial step in dictating their forward trafficking to the functional destinations which in turn controls the magnitude and duration of receptor-elicited cellular response, and defects in GPCR export from the ER are directly associated with the pathogenesis of human diseases.<sup>11,70-73</sup> AT2R and AT1R mediate the function of Ang II which plays an important role in the maintenance of blood pressure and fluid homeostasis.<sup>74</sup> Although AT1R has been thought to mediate the most physiological actions of Ang II and AT2R is a counter-regulator of AT1R actions, recent studies indicate that AT2R has protective functions in a variety of diseases and is a potential therapeutic target for hypertension and obesity.<sup>74</sup> CXCR4 regulates a wide range of cellular processes, such as migration, tumor growth, metastasis, and homing of immune cells to the sites of inflammation and injury, and its antagonists inhibit cancer progression.<sup>75-77</sup> We have demonstrated here that Ang II receptors and CXCR4 are actively recruited to COPII vesicles via specific motifs and this process plays an important role in receptor forward delivery. However, physiological and/or pathological functions of COPII-mediated concentration of these receptors need further investigation. Nevertheless, our data presented in this paper reveal the molecular mechanisms of nascent GPCR targeting to COPII vesicles and provide important insights into regulation of GPCR transport along the biosynthetic pathways, as well as regulation of general vesicle-mediated membrane trafficking.

### Limitations of the study

Future work needs to study the COPII vesicle targeting of GPCRs at endogenous levels in cell lines.

### STAR★METHODS

Detailed methods are provided in the online version of this paper and include the following:

- [KEY RESOURCES TABLE](#)
- [RESOURCE AVAILABILITY](#)
  - Lead contact
  - Materials availability

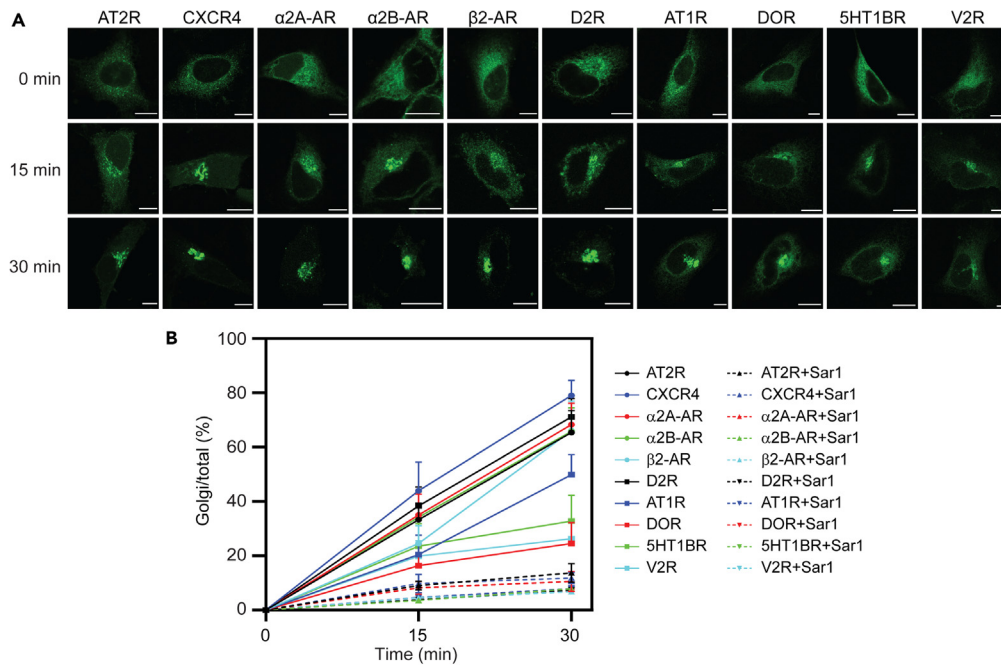


**Figure 7. Comparison of the ER-Golgi export of different GPCRs and the effect of Sar1H79G**

(A) Representative images showing the ER-Golgi export of GPCRs.

(B) Quantitative data of the ER-Golgi transport of GPCRs as shown in (A) and Sar1H79G inhibition. HeLa cells were transfected with RUSH plasmids expressing individual GPCRs for 20 h and then incubated with biotin for 15 and 30 min. The highly concentrated cargo molecules in the perinuclear region were measured as their expression at the Golgi. The quantitative data are expressed as the ratio of the Golgi expression to the total expression. The data are mean  $\pm$  SD (n = 40–50 cells in at least 4 experiments). Scale bars, 10  $\mu$ m.

- Data and code availability
- EXPERIMENTAL MODEL AND STUDY PARTICIPANT**
- Cell culture
- METHOD DETAILS**
- Plasmids and constructions

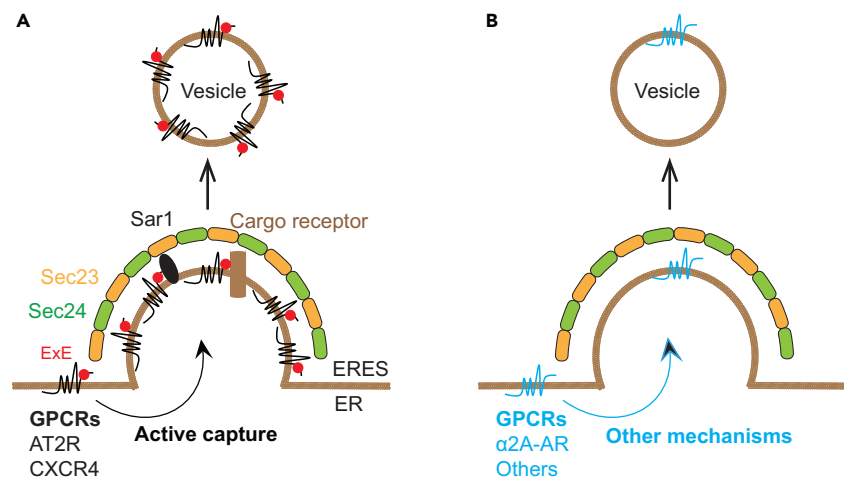


**Figure 8. Models of GPCR recruitment to the ERES for export from the ER via COPII vesicles**

(A) Some GPCR members, such as AT2R and CXCR4, are actively captured by COPII vesicles. AT2R recruitment to COPII vesicles may be directed by interaction with Sar1 and the C-terminal ExE motif that may mediate receptor interaction with yet identified regulatory proteins or a cargo receptor.

(B) Most GPCRs, such as  $\alpha_{2A}$ -AR, use other mechanisms for loading to COPII vesicles.

- Transient transfection
- RUSH assays
- Fluorescence microscopy
- Nano-Glo HiBiT extracellular detection assays
- GST fusion protein pulldown assays
- Co-IP
- **QUANTIFICATION AND STATISTICAL ANALYSIS**

## SUPPLEMENTAL INFORMATION

Supplemental information can be found online at <https://doi.org/10.1016/j.isci.2023.107969>.

## ACKNOWLEDGMENTS

This work was supported by the National Institutes of Health grants R35GM145284 to N.A.L. and R35GM136397 to G.W.

## AUTHOR CONTRIBUTIONS

X.X., N.A.L., and G.W. conceived and designed the experiments. X.X. and G.W. performed the experiments. X.X. and G.W. analyzed the results. X.X., N.A.L., and G.W. wrote the manuscript.

## DECLARATION OF INTERESTS

G.W. is a member of the editorial advisory board for iScience and played no role in the review and editorial handling of this paper.

Received: March 30, 2023

Revised: June 2, 2023

Accepted: September 15, 2023

Published: September 19, 2023

## REFERENCES

1. Pierce, K.L., Premont, R.T., and Lefkowitz, R.J. (2002). Seven-transmembrane receptors. *Nat. Rev. Mol. Cell Biol.* 3, 639–650. <https://doi.org/10.1038/nrm908>.
2. Yang, D., Zhou, Q., Labroska, V., Qin, S., Darbalaei, S., Wu, Y., Yuliantie, E., Xie, L., Tao, H., Cheng, J., et al. (2021). G protein-coupled receptors: structure- and function-based drug discovery. *Signal Transduct. Target. Ther.* 6, 7. <https://doi.org/10.1038/s41392-020-00435-w>.
3. Xu, X., and Wu, G. (2023). Non-canonical Golgi-compartmentalized Gbetagamma signaling: mechanisms, functions, and therapeutic targets. *Trends Pharmacol. Sci.* 44, 98–111. <https://doi.org/10.1016/j.tips.2022.11.003>.
4. Jang, W., Lu, S., Xu, X., Wu, G., and Lambert, N.A. (2023). The role of G protein conformation in receptor-G protein selectivity. *Nat. Chem. Biol.* 19, 687–694. <https://doi.org/10.1038/s41589-022-01231-z>.
5. Jiang, H., Galtes, D., Wang, J., and Rockman, H.A. (2022). G protein-coupled receptor signaling: transducers and effectors. *Am. J. Physiol. Cell Physiol.* 323, C731–C748. <https://doi.org/10.1152/ajpcell.00210.2022>.
6. Li, C., Wei, Z., Fan, Y., Huang, W., Su, Y., Li, H., Dong, Z., Fukuda, M., Khater, M., and Wu, G. (2017). The GTPase Rab43 controls the anterograde ER-Golgi trafficking and sorting of GPCRs. *Cell Rep.* 21, 1089–1101. <https://doi.org/10.1016/j.celrep.2017.10.011>.
7. Wu, G., Benovic, J.L., Hildebrandt, J.D., and Lanier, S.M. (1998). Receptor docking sites for G-protein betagamma subunits. Implications for signal regulation. *J. Biol. Chem.* 273, 7197–7200.
8. Wu, G., Bogatkevich, G.S., Mukhin, Y.V., Benovic, J.L., Hildebrandt, J.D., and Lanier, S.M. (2000). Identification of Gbetagamma binding sites in the third intracellular loop of the M(3)-muscarinic receptor and their role in receptor regulation. *J. Biol. Chem.* 275, 9026–9034.
9. Duvernay, M.T., Wang, H., Dong, C., Guidry, J.J., Sackett, D.L., and Wu, G. (2011). Alpha2B-adrenergic receptor interaction with tubulin controls its transport from the endoplasmic reticulum to the cell surface. *J. Biol. Chem.* 286, 14080–14089. <https://doi.org/10.1074/jbc.M111.223233>.
10. Dong, C., Filipeanu, C.M., Duvernay, M.T., and Wu, G. (2007). Regulation of G protein-coupled receptor export trafficking. *Biochim. Biophys. Acta* 1768, 853–870. <https://doi.org/10.1016/j.bbame.2006.09.008>.
11. Zhang, M., and Wu, G. (2019). Mechanisms of the anterograde trafficking of GPCRs: Regulation of AT1R transport by interacting proteins and motifs. *Traffic* 20, 110–120. <https://doi.org/10.1111/tra.12624>.
12. Tai, A.W., Chuang, J.Z., Bode, C., Wolfrum, U., and Sung, C.H. (1999). Rhodopsin's carboxy-terminal cytoplasmic tail acts as a membrane receptor for cytoplasmic dynein by binding to the dynein light chain Tctex-1. *Cell* 97, 877–887.
13. McLatchie, L.M., Fraser, N.J., Main, M.J., Wise, A., Brown, J., Thompson, N., Solari, R., Lee, M.G., and Foord, S.M. (1998). RAMPs regulate the transport and ligand specificity of the calcitonin-receptor-like receptor. *Nature* 393, 333–339. <https://doi.org/10.1038/30666>.
14. Colley, N.J., Baker, E.K., Starnes, M.A., and Zuker, C.S. (1991). The cyclophilin homolog ninaA is required in the secretory pathway. *Cell* 67, 255–263.
15. Ferreira, P.A., Nakayama, T.A., Pak, W.L., and Travis, G.H. (1996). Cyclophilin-related protein RanBP2 acts as chaperone for red/green opsin. *Nature* 383, 637–640. <https://doi.org/10.1038/383637a0>.
16. Sauvageau, E., Rochdi, M.D., Oueslati, M., Hamdan, F.F., Percherancier, Y., Simpson, J.C., Pepperkok, R., and Bouvier, M. (2014). CNIH4 interacts with newly synthesized GPCR and controls their export from the endoplasmic reticulum. *Traffic* 15, 383–400. <https://doi.org/10.1111/tra.12148>.
17. Shiwarski, D.J., Darr, M., Telmer, C.A., Bruchez, M.P., and Puthenveedu, M.A. (2017). PI3K class II alpha regulates delta-opioid receptor export from the trans-Golgi network. *Mol. Biol. Cell* 28, 2202–2219. <https://doi.org/10.1091/mbc.E17-01-0030>.
18. Al Awabdh, S., Miserey-Lenkei, S., Bouceba, T., Masson, J., Kano, F., Marinach-Patrice, C., Hamon, M., Emerit, M.B., and Darmon, M. (2012). A new vesicular scaffolding complex mediates the G-protein-coupled 5-HT1A receptor targeting to neuronal dendrites. *J. Neurosci.* 32, 14227–14241. <https://doi.org/10.1523/JNEUROSCI.6329-11.2012>.
19. Wei, Z., Xu, X., Fang, Y., Khater, M., Naughton, S.X., Hu, G., Terry, A.V., Jr., and Wu, G. (2021). Rab43 GTPase directs postsynaptic trafficking and neuron-specific sorting of G protein-coupled receptors. *J. Biol. Chem.* 296, 100517. <https://doi.org/10.1016/j.jbc.2021.100517>.

20. Wei, Z., Zhang, M., Li, C., Huang, W., Fan, Y., Guo, J., Khater, M., Fukuda, M., Dong, Z., Hu, G., and Wu, G. (2019). Specific TBC domain-containing proteins control the ER-Golgi-plasma membrane trafficking of GPCRs. *Cell Rep.* 28, 554–566.e4. <https://doi.org/10.1016/j.celrep.2019.05.033>.
21. Dwyer, N.D., Troemel, E.R., Sengupta, P., and Bargmann, C.I. (1998). Odorant receptor localization to olfactory cilia is mediated by ODR-4, a novel membrane-associated protein. *Cell* 93, 455–466.
22. Li, C., Fan, Y., Lan, T.H., Lambert, N.A., and Wu, G. (2012). Rab26 modulates the cell surface transport of alpha2-adrenergic receptors from the Golgi. *J. Biol. Chem.* 287, 42784–42794. <https://doi.org/10.1074/jbc.M112.410936>.
23. Wu, G., Zhao, G., and He, Y. (2003). Distinct pathways for the trafficking of angiotensin II and adrenergic receptors from the endoplasmic reticulum to the cell surface: Rab1-independent transport of a G protein-coupled receptor. *J. Biol. Chem.* 278, 47062–47069. <https://doi.org/10.1074/jbc.M305707200>.
24. Filipeanu, C.M., Zhou, F., Claycomb, W.C., and Wu, G. (2004). Regulation of the cell surface expression and function of angiotensin II type 1 receptor by Rab1-mediated endoplasmic reticulum-to-Golgi transport in cardiac myocytes. *J. Biol. Chem.* 279, 41077–41084. <https://doi.org/10.1074/jbc.M405988200>.
25. Zhang, M., Davis, J.E., Li, C., Gao, J., Huang, W., Lambert, N.A., Terry, A.V., Jr., and Wu, G. (2016). GGA3 interacts with a G protein-coupled receptor and modulates its cell surface export. *Mol. Cell Biol.* 36, 1152–1163. <https://doi.org/10.1128/mcb.00009-16>.
26. Doly, S., Shirvani, H., Gäta, C., Meye, F.J., Emerit, M.B., Enslin, H., Achour, L., Pardo-Lopez, L., Yang, S.K., Armand, V., et al. (2016). GABAB receptor cell-surface export is controlled by an endoplasmic reticulum gatekeeper. *Mol. Psychiatry* 21, 480–490. <https://doi.org/10.1038/mp.2015.72>.
27. Xu, X., and Wu, G. (2022). Human C1orf27 protein interacts with alpha(2A)-adrenergic receptor and regulates its anterograde transport. *J. Biol. Chem.* 298, 102021. <https://doi.org/10.1016/j.jbc.2022.102021>.
28. Lee, M.C.S., Miller, E.A., Goldberg, J., Orci, L., and Schekman, R. (2004). Bi-directional protein transport between the ER and Golgi. *Annu Rev. Cell Dev. Bi.* 20, 87–123. <https://doi.org/10.1146/annurev.cellbio.20.010403.105307>.
29. Gürkan, C., Stagg, S.M., Lapointe, P., and Balch, W.E. (2006). The COPII cage: unifying principles of vesicle coat assembly. *Nat. Rev. Mol. Cell Biol.* 7, 727–738. <https://doi.org/10.1038/nrm2025>.
30. Fath, S., Mancias, J.D., Bi, X., and Goldberg, J. (2007). Structure and organization of coat proteins in the COPII cage. *Cell* 129, 1325–1336. <https://doi.org/10.1016/j.cell.2007.05.036>.
31. Weigel, A.V., Chang, C.L., Shtengel, G., Xu, C.S., Hoffman, D.P., Freeman, M., Iyer, N., Aaron, J., Khoun, S., Bogovic, J., et al. (2021). ER-to-Golgi protein delivery through an interwoven, tubular network extending from ER. *Cell* 184, 2412–2429.e16. <https://doi.org/10.1016/j.cell.2021.03.035>.
32. Westrate, L.M., Hoyer, M.J., Nash, M.J., and Voeltz, G.K. (2020). Vesicular and uncoated Rab1-dependent cargo carriers facilitate ER to Golgi transport. *J. Cell Sci.* 133, jcs.239814. <https://doi.org/10.1242/jcs.239814>.
33. Shomron, O., Nevo-Yassaf, I., Aviad, T., Yaffe, Y., Zahavi, E.E., Dukhovny, A., Perlson, E., Brodsky, I., Yeheskel, A., Pasmanik-Chor, M., et al. (2021). COPII collar defines the boundary between ER and ER exit site and does not coat cargo containers. *J. Cell Biol.* 220, e201907224. <https://doi.org/10.1083/jcb.201907224>.
34. Chatterjee, S., Choi, A.J., and Frankel, G. (2021). A systematic review of Sec24 cargo interactome. *Traffic* 22, 412–424. <https://doi.org/10.1111/tra.12817>.
35. Kuehn, M.J., Herrmann, J.M., and Schekman, R. (1998). COPII-cargo interactions direct protein sorting into ER-derived transport vesicles. *Nature* 391, 187–190. <https://doi.org/10.1038/34438>.
36. Malkus, P., Jiang, F., and Schekman, R. (2002). Concentrative sorting of secretory cargo proteins into COPII-coated vesicles. *J. Cell Biol.* 159, 915–921. <https://doi.org/10.1083/jcb.200208074>.
37. Balch, W.E., McCaffery, J.M., Plutner, H., and Farquhar, M.G. (1994). Vesicular stomatitis virus glycoprotein is sorted and concentrated during export from the endoplasmic reticulum. *Cell* 76, 841–852. [https://doi.org/10.1016/0092-8674\(94\)90359-x](https://doi.org/10.1016/0092-8674(94)90359-x).
38. Nishimura, N., and Balch, W.E. (1997). A di-acidic signal required for selective export from the endoplasmic reticulum. *Science* 277, 556–558.
39. Miller, E., Antony, B., Hamamoto, S., and Schekman, R. (2002). Cargo selection into COPII vesicles is driven by the Sec24p subunit. *EMBO J.* 21, 6105–6113. <https://doi.org/10.1093/emboj/cdf605>.
40. Bonnon, C., Wendeler, M.W., Paccaud, J.P., and Hauri, H.P. (2010). Selective export of human GPI-anchored proteins from the endoplasmic reticulum. *J. Cell Sci.* 123, 1705–1715. <https://doi.org/10.1242/jcs.062950>.
41. Wendeler, M.W., Paccaud, J.P., and Hauri, H.P. (2007). Role of Sec24 isoforms in selective export of membrane proteins from the endoplasmic reticulum. *EMBO Rep.* 8, 258–264. <https://doi.org/10.1038/sj.embor.7400893>.
42. Miller, E.A., Beilharz, T.H., Malkus, P.N., Lee, M.C.S., Hamamoto, S., Orci, L., and Schekman, R. (2003). Multiple cargo binding sites on the COPII subunit Sec24p ensure capture of diverse membrane proteins into transport vesicles. *Cell* 114, 497–509. [https://doi.org/10.1016/s0092-8674\(03\)00609-3](https://doi.org/10.1016/s0092-8674(03)00609-3).
43. Sevier, C.S., Weisz, O.A., Davis, M., and Machamer, C.E. (2000). Efficient export of the vesicular stomatitis virus G protein from the endoplasmic reticulum requires a signal in the cytoplasmic tail that includes both tyrosine-based and di-acidic motifs. *Mol. Biol. Cell* 11, 13–22.
44. Zuzarte, M., Rinné, S., Schlichthörl, G., Schubert, A., Daut, J., and Preisig-Müller, R. (2007). A di-acidic sequence motif enhances the surface expression of the potassium channel TASK-3. *Traffic* 8, 1093–1100.
45. Wang, X., Matteson, J., An, Y., Moyer, B., Yoo, J.S., Bannykh, S., Wilson, I.A., Riordan, J.R., and Balch, W.E. (2004). COPII-dependent export of cystic fibrosis transmembrane conductance regulator from the ER uses a di-acidic exit code. *J. Cell Biol.* 167, 65–74.
46. Martínez-Mármol, R., Pérez-Verdaguer, M., Roig, S.R., Vallejo-Gracia, A., Gotsi, P., Serrano-Albarrás, A., Bahamonde, M.I., Ferrer-Montiel, A., Fernández-Ballester, G., Comes, N., and Felipe, A. (2013). A non-canonical di-acidic signal at the C-terminus of Kv1.3 determines anterograde trafficking and surface expression. *J. Cell Sci.* 126, 5681–5691. <https://doi.org/10.1242/jcs.134825>.
47. Zhuang, X., Chowdhury, S., Northrup, J.K., and Ray, K. (2010). Sar1-dependent trafficking of the human calcium receptor to the cell surface. *Biochem. Biophys. Res. Commun.* 396, 874–880. <https://doi.org/10.1016/j.bbrc.2010.05.014>.
48. Dong, C., Zhou, F., Fugetta, E.K., Filipeanu, C.M., and Wu, G. (2008). Endoplasmic reticulum export of adrenergic and angiotensin II receptors is differentially regulated by Sar1 GTPase. *Cell. Signal.* 20, 1035–1043. <https://doi.org/10.1016/j.cellsig.2008.01.014>.
49. Walther, C., Lotze, J., Beck-Sickinger, A.G., and Mörl, K. (2012). The anterograde transport of the human neuropeptide Y2 receptor is regulated by a subtype specific mechanism mediated by the C-terminus. *Neuropeptides* 46, 335–343. <https://doi.org/10.1016/j.npep.2012.08.011>.
50. Dong, C., Nichols, C.D., Guo, J., Huang, W., Lambert, N.A., and Wu, G. (2012). A triple arg motif mediates alpha(2B)-adrenergic receptor interaction with Sec24C/D and export. *Traffic* 13, 857–868. <https://doi.org/10.1111/j.1600-0854.2012.01351.x>.
51. Zhang, X., Dong, C., Wu, Q.J., Balch, W.E., and Wu, G. (2011). Di-acidic motifs in the membrane-distal C termini modulate the transport of angiotensin II receptors from the endoplasmic reticulum to the cell surface. *J. Biol. Chem.* 286, 20525–20535. <https://doi.org/10.1074/jbc.M111.222034>.
52. Duvernay, M.T., Dong, C., Zhang, X., Robitaille, M., Hébert, T.E., and Wu, G. (2009). A single conserved leucine residue on the first intracellular loop regulates ER export of G protein-coupled receptors. *Traffic* 10, 552–566. <https://doi.org/10.1111/j.1600-0854.2009.00890.x>.
53. Dong, C., and Wu, G. (2006). Regulation of anterograde transport of alpha2-adrenergic receptors by the N termini at multiple intracellular compartments. *J. Biol. Chem.* 281, 38543–38554. <https://doi.org/10.1074/jbc.M605734200>.
54. Shiwarski, D.J., Crilly, S.E., Dates, A., and Puthenveedu, M.A. (2019). Dual RXR motifs regulate nerve growth factor-mediated intracellular retention of the delta opioid receptor. *Mol. Biol. Cell* 30, 680–690. <https://doi.org/10.1091/mbc.E18-05-0292>.
55. Schüle, R., Hermosilla, R., Oksche, A., Dehe, M., Wiesner, B., Krause, G., and Rosenthal, W. (1998). A dileucine sequence and an upstream glutamate residue in the intracellular carboxyl terminus of the vasopressin V2 receptor are essential for cell surface transport in COS.M6 cells. *Mol. Pharmacol.* 54, 525–535. <https://doi.org/10.1124/mol.54.3.525>.
56. Bermak, J.C., Li, M., Bullock, C., and Zhou, Q.Y. (2001). Regulation of transport of the dopamine D1 receptor by a new membrane-associated ER protein. *Nat. Cell Biol.* 3, 492–498. <https://doi.org/10.1038/35074561>.
57. Duvernay, M.T., Dong, C., Zhang, X., Zhou, F., Nichols, C.D., and Wu, G. (2009). Anterograde trafficking of G protein-coupled receptors: function of the C-terminal F(X)6LL motif in export from the endoplasmic reticulum. *Mol. Pharmacol.* 75, 751–761. <https://doi.org/10.1124/mol.108.051623>.

58. Duvernay, M.T., Zhou, F., and Wu, G. (2004). A conserved motif for the transport of G protein-coupled receptors from the endoplasmic reticulum to the cell surface. *J. Biol. Chem.* 279, 30741–30750. <https://doi.org/10.1074/jbc.M313881200>.
59. Xu, X., Wei, Z., and Wu, G. (2022). Specific motifs mediate post-synaptic and surface transport of G protein-coupled receptors. *iScience* 25, 103643. <https://doi.org/10.1016/j.isci.2021.103643>.
60. Carrel, D., Hamon, M., and Darmon, M. (2006). Role of the C-terminal di-leucine motif of 5-HT1A and 5-HT1B serotonin receptors in plasma membrane targeting. *J. Cell Sci.* 119, 4276–4284. <https://doi.org/10.1242/jcs.03189>.
61. Zhang, S., Xue, L., Liu, X., Zhang, X.C., Zhou, R., Zhao, H., Shen, C., Pin, J.P., Rondard, P., and Liu, J. (2020). Structural basis for distinct quality control mechanisms of GABA(B) receptor during evolution. *FASEB J* 34, 16348–16363. <https://doi.org/10.1096/fj.202001355RR>.
62. Boncompain, G., Divoux, S., Gareil, N., de Forges, H., Lescure, A., Latreche, L., Mercanti, V., Jollivet, F., Raposo, G., and Perez, F. (2012). Synchronization of secretory protein traffic in populations of cells. *Nat. Methods* 9, 493–498. <https://doi.org/10.1038/nmeth.1928>.
63. Giraud, C.G., and Maccioni, H.J.F. (2003). Endoplasmic reticulum export of glycosyltransferases depends on interaction of a cytoplasmic dibasic motif with Sar1. *Mol. Biol. Cell* 14, 3753–3766. <https://doi.org/10.1091/mbc.e03-02-0101>.
64. Okamoto, Y., Bernstein, J.D., and Shikano, S. (2013). Role of C-terminal membrane-proximal basic residues in cell surface trafficking of HIV coreceptor GPR15 protein. *J. Biol. Chem.* 288, 9189–9199. <https://doi.org/10.1074/jbc.M112.445817>.
65. Barlowe, C., and Helenius, A. (2016). Cargo Capture and Bulk Flow in the Early Secretory Pathway. *Annu. Rev. Cell Dev. Biol.* 32, 197–222. <https://doi.org/10.1146/annurev-cellbio-111315-125016>.
66. Wieland, F.T., Gleason, M.L., Serafini, T.A., and Rothman, J.E. (1987). The rate of bulk flow from the endoplasmic reticulum to the cell surface. *Cell* 50, 289–300. [https://doi.org/10.1016/0092-8674\(87\)90224-8](https://doi.org/10.1016/0092-8674(87)90224-8).
67. Liebmann, T., Kruusmägi, M., Sourial-Bassillious, N., Bondar, A., Svenningsson, P., Flajole, M., Greengard, P., Scott, L., Brismar, H., and Aperia, A. (2012). A noncanonical postsynaptic transport route for a GPCR belonging to the serotonin receptor family. *J. Neurosci.* 32, 17998–18008. <https://doi.org/10.1523/JNEUROSCI.1804-12.2012>.
68. Wu, B., Chien, E.Y.T., Mol, C.D., Fenalti, G., Liu, W., Katritch, V., Abagyan, R., Brooun, A., Wells, P., Bi, F.C., et al. (2010). Structures of the CXCR4 chemokine GPCR with small-molecule and cyclic peptide antagonists. *Science* 330, 1066–1071. <https://doi.org/10.1126/science.1194396>.
69. Wruck, C.J., Funke-Kaiser, H., Pufe, T., Kusserow, H., Menk, M., Scheff, J.H., Kruse, M.L., Stoll, M., and Unger, T. (2005). Regulation of transport of the angiotensin AT2 receptor by a novel membrane-associated Golgi protein. *Arterioscler. Thromb. Vasc. Biol.* 25, 57–64. <https://doi.org/10.1161/01.ATV.0000150662.51436.14>.
70. Conn, P.M., Ulloa-Aguirre, A., Ito, J., and Janovick, J.A. (2007). G protein-coupled receptor trafficking in health and disease: lessons learned to prepare for therapeutic mutant rescue in vivo. *Pharmacol. Rev.* 59, 225–250. <https://doi.org/10.1124/pr.59.3.2>.
71. Wang, G., and Wu, G. (2012). Small GTPase regulation of GPCR anterograde trafficking. *Trends Pharmacol. Sci.* 33, 28–34. <https://doi.org/10.1016/j.tips.2011.09.002>.
72. Ulloa-Aguirre, A., Zariñán, T., Gutiérrez-Sagal, R., and Tao, Y.X. (2022). Targeting trafficking as a therapeutic avenue for misfolded GPCRs leading to endocrine diseases. *Front. Endocrinol.* 13, 934685. <https://doi.org/10.3389/fendo.2022.934685>.
73. Kunduri, G., Yuan, C., Parthibane, V., Nyswaner, K.M., Kanwar, R., Nagashima, K., Britt, S.G., Mehta, N., Kotu, V., Porterfield, M., et al. (2014). Phosphatidic acid phospholipase A1 mediates ER-Golgi transit of a family of G protein-coupled receptors. *J. Cell Biol.* 206, 79–95. <https://doi.org/10.1083/jcb.201405020>.
74. Steckelings, U.M., Widdop, R.E., Sturrock, E.D., Lubbe, L., Hussain, T., Kaschina, E., Unger, T., Hallberg, A., Carey, R.M., and Summers, C. (2022). The Angiotensin AT(2) Receptor: From a Binding Site to a Novel Therapeutic Target. *Pharmacol. Rev.* 74, 1051–1135. <https://doi.org/10.1124/pharmrev.120.000281>.
75. Khater, M., Bryant, C.N., and Wu, G. (2021). Gbetagamma translocation to the Golgi apparatus activates ARF1 to spatiotemporally regulate G protein-coupled receptor signaling to MAPK. *J. Biol. Chem.* 296, 100805. <https://doi.org/10.1016/j.jbc.2021.100805>.
76. Khater, M., Wei, Z., Xu, X., Huang, W., Lokeshwar, B.L., Lambert, N.A., and Wu, G. (2021). G protein betagamma translocation to the Golgi apparatus activates MAPK via p110gamma-p101 heterodimers. *J. Biol. Chem.* 296, 100325. <https://doi.org/10.1016/j.jbc.2021.100325>.
77. Chatterjee, S., Behnam Azad, B., and Nimmagadda, S. (2014). The intricate role of CXCR4 in cancer. *Adv. Cancer Res.* 124, 31–82. <https://doi.org/10.1016/B978-0-12-411638-2.00002-1>.
78. Ward, T.H., Polishchuk, R.S., Caplan, S., Hirschberg, K., and Lippincott-Schwartz, J. (2001). Maintenance of Golgi structure and function depends on the integrity of ER export. *J. Cell Biol.* 155, 557–570. <https://doi.org/10.1083/jcb.200107045>.
79. Lan, T.H., Liu, Q., Li, C., Wu, G., and Lambert, N.A. (2012). Sensitive and high resolution localization and tracking of membrane proteins in live cells with BRET. *Traffic* 13, 1450–1456. <https://doi.org/10.1111/j.1600-0854.2012.01401.x>.
80. Cole, N.B., Smith, C.L., Sciaky, N., Terasaki, M., Edidin, M., and Lippincott-Schwartz, J. (1996). Diffusional mobility of Golgi proteins in membranes of living cells. *Science* 273, 797–801. <https://doi.org/10.1126/science.273.5276.797>.
81. Kroeze, W.K., Sassano, M.F., Huang, X.P., Lansu, K., McCorry, J.D., Giguère, P.M., Sciaky, N., and Roth, B.L. (2015). PRESTO-Tango as an open-source resource for interrogation of the druggable human GPCRome. *Nat. Struct. Mol. Biol.* 22, 362–369. <https://doi.org/10.1038/nsmb.3014>.

STAR★METHODS

KEY RESOURCES TABLE

REAGENT or RESOURCE	SOURCE	IDENTIFIER
<b>Antibodies</b>		
Mouse monoclonal anti-GFP (clone B-2)	Santa Cruz Biotechnology	Cat# sc-9996; RRID: AB_627695
Rabbit monoclonal anti-HA	Cell Signaling Technology	Cat# 3724; RRID: AB_1549585
Mouse monoclonal anti-HA (clone 12CA5)	Roche	Cat# 11583816001; RRID: AB_1549585
<b>Chemicals, peptides, and recombinant proteins</b>		
D-biotin	Thermo Fisher Scientific	Cat# AC230090010
Cycloheximide	Thermo Fisher Scientific	Cat# AAJ6690103
Polyethylenimine	Polysciences	Cat# 23966
Dynabeads™ protein G	Invitrogen	Cat# 10004D
ProLong gold antifade mountant with DAPI	Invitrogen	Cat# P36931
MagneGST™ glutathione particles	Promega	Cat# V8611
Nano-Glo HiBiT Extracellular Detection System	Promega	Cat# N2420
Dulbecco's modified Eagles medium	HyClone	Cat# SH30243.01HI
Fetal bovine serum	HyClone	Cat# SH30396.03HI
QuikChange II XL site-directed mutagenesis kit	Agilent	Cat# 200521
<b>Experimental models: Cell lines</b>		
HEK293	ATCC	Cat# CRL-1573
HeLa	ATCC	Cat# CRM-CCL-2
<b>Recombinant DNA</b>		
Str-KDEL_SBP-EGFP-Ecadherin	Addgene	Cat# 65286
Str-KDEL_SBP-EGFP-VSVG	This paper	N/A
Str-KDEL_SBP-EGFP-VSVG-DxE-AxA	This paper	N/A
Str-KDEL_SBP-EGFP-AT2R	This paper	N/A
Str-KDEL_SBP-EGFP-AT2R -ExE-AxA	This paper	N/A
Str-KDEL_SBP-EGFP-AT1R	This paper	N/A
Str-KDEL_SBP-EGFP-CXCR4	This paper	N/A
Str-KDEL_SBP-EGFP-CXCR4-ExE-AxA	This paper	N/A
Str-KDEL_SBP-EGFP-CXCR4-KxKR-AxAA	This paper	N/A
Str-KDEL_SBP-EGFP-CXCR4(1-322)	This paper	N/A
Str-KDEL_SBP-EGFP-CXCR4(1-313)	This paper	N/A
Str-KDEL_SBP-EGFP-CXCR4(1-302)	This paper	N/A
Str-KDEL_SBP-EGFP- $\alpha_{2A}$ -AR	Xu and Wu <sup>27</sup>	N/A
Str-KDEL_SBP-EGFP- $\alpha_{2B}$ -AR	This paper	N/A
Str-KDEL_SBP-EGFP- $\beta_2$ -AR	Xu and Wu <sup>27</sup>	N/A
Str-KDEL_SBP-EGFP-D2R	Xu and Wu <sup>27</sup>	N/A
Str-KDEL_SBP-M3R-EGFP	This paper	N/A
Str-KDEL_SBP-EGFP-A2AR	This paper	N/A
Str-KDEL_SBP-EGFP-DOR	This paper	N/A
Str-KDEL_SBP-EGFP-5HT1BR	This paper	N/A
Str-KDEL_SBP-EGFP-V2R	This paper	N/A
Str-KDEL_SBP-mCherry-AT2R	This paper	N/A
Str-KDEL_SBP-HiBiT-EGFP-AT2R	This paper	N/A

(Continued on next page)

**Continued**

REAGENT or RESOURCE	SOURCE	IDENTIFIER
3HA-AT2R	Zhang et al. <sup>51</sup>	N/A
3HA-AT2R-ExE-AxA	Zhang et al. <sup>51</sup>	N/A
GST-AT2Rct	This paper	N/A
GST-AT2Rct-ExE-AxA	This paper	N/A
GFP-Sec24A	Dong et al. <sup>50</sup>	N/A
GFP-Sec24B	Dong et al. <sup>50</sup>	N/A
GFP-Sec24C	Dong et al. <sup>50</sup>	N/A
GFP-Sec24D	Dong et al. <sup>50</sup>	N/A
GFP-Sec23A	Li et al. <sup>6</sup>	N/A
GFP-Sec23B	Li et al. <sup>6</sup>	N/A
GFP-Sec16	Addgene	Cat# 36155
GFP-Sar1	This paper	N/A
DsRed-Sar1H79G	This paper	N/A
Myc-Sar1	This paper	N/A
DsRed-Sec24D	This paper	N/A
p58-YFP	Ward et al. <sup>78</sup>	
Venus-giantin	Lan et al. <sup>79</sup>	
YFP-GalT	Cole et al. <sup>80</sup>	
pmTurquoise2-GalT	Khater et al. <sup>76</sup>	
<b>Software and algorithms</b>		
ImageJ	NIH	<a href="https://imagej.nih.gov/ij/">ImageJ.nih.gov/ij/</a>
Las X 4.3.0	Leica Microsystems	<a href="https://www.leica-microsystems.com">Leica-microsystems.com</a>

## RESOURCE AVAILABILITY

### Lead contact

Further information and requests for resources and reagents should be directed to and will be fulfilled by the Lead Contact: Guangyu Wu ([guwu@augusta.edu](mailto:guwu@augusta.edu)).

### Materials availability

Reagents generated in this study are available from the [lead contact](#) upon request.

### Data and code availability

- All data reported in this paper will be available from the [lead contact](#) upon request.
- This paper does not report original code.
- Any additional information reported in this paper will be shared by the [lead contact](#) upon request.

## EXPERIMENTAL MODEL AND STUDY PARTICIPANT

### Cell culture

HeLa and HEK293 cells were cultured in Dulbecco's modified Eagle's medium (DMEM) with 10% fetal bovine serum (FBS), 100 units/ml penicillin and 100 µg/mL streptomycin.

## METHOD DETAILS

### Plasmids and constructions

GPCR plasmids in PRESTO-Tango kits were from Addgene (#1000000068) as described.<sup>81</sup> The 3HA-tagged human AT2R and its ExE-AxA mutant in pcDNA3.1 vectors, GFP-tagged Sec24 in pEGFP-C3 vectors and the RUSH plasmids of  $\alpha_{2A}$ -AR,  $\beta_2$ -AR and D2R were generated as described previously.<sup>27,50,51</sup> To generate the RUSH plasmid Str-KDEL\_SBP-EGFP-VSVG, VSVG without signal peptide was amplified by PCR using primers (Table S1), digested with FseI and XbaI enzymes and then ligated to the plasmid Str-KDEL\_SBP-EGFP-Ecadherin (Addgene

#65286<sup>62</sup> which was digested with the same enzymes to release ecadherin. The similar strategy was used to generate the RUSH plasmids expressing AT2R, AT1R, CXCR4,  $\alpha_{2B}$ -AR, A2AR, DOR and 5HT1BR using primers. To generate the RUSH plasmid Str-KDEL\_SBP-M3R-EGFP, M3R-EGFP in pEGFP-N1 vectors was first mutated to remove the Sdal restriction site by QuickChange site-directed mutagenesis using primers, amplified by PCR using primers, digested with Sdal and XbaI and ligated into the plasmid Str-KDEL\_SBP-EGFP-Ecadherin which was digested with the same enzymes to release ecadherin. To generate Str-KDEL\_SBP-V2R-EGFP, V2R was amplified by PCR using primers, digested with Sdal and BamHI and ligated into the plasmid Str-KDEL\_SBP-M3R-EGFP which was digested with the same enzymes to release M3R. The RUSH plasmids expressing cargo mutants were generated by QuickChange site-directed mutagenesis kits using wild type RUSH plasmids as templates, including VSVG DxE-AxA mutant, CXCR4 ExE-AxA mutant and CXCR4 KxKR-AxA mutant. To generate the RUSH plasmid expressing AT2R ExE-AxA mutant, 3HA-tagged AT2R ExE-AxA mutant in pcDNA3.1 vectors was amplified by PCR using primers and then cloned into Str-KDEL\_SBP-EGFP-AT2R after digestion with FseI and XbaI enzymes to release AT2R. To generate the RUSH plasmids containing truncated CXCR4, CXCR4 fragments (1–322, 1–313 and 1–302) were amplified by PCR using primers and ligated to the plasmid Str-KDEL\_SBP-EGFP-CXCR4 after digestion to release CXCR4. To insert HiBit between SBP and EGFP in the RUSH plasmids expressing AT2R or its EXE-AxA mutant, double-stranded DNA coding SBP and HiBiT (GAATCCGACGAGAAGACCACTGGTTGGCGAGGTGGACACG TTGTTGAAGGACTGGCTGGGGAACCTGAACAACCTTCGTGCACGACTGGAGCATCACCCACAAGGTCAACGTGAACCAGGCGGAGTGTC CGGCTGGCGGCTGTTCAAGAAGATTCTGGAGGCCCTGCAGG) was synthesized, digested with EcoRI and Sdal, and then cloned into the plasmids after digestion with the same enzymes. To generate GST fusion protein constructs coding AT2Rct and its ExE-AxA mutant, the C-terminus was amplified by PCR using full length AT2R and its ExE-AxA mutant in pcDNA3.1 vectors as templates and primers and then cloned into pGEX-4T-1 vectors at BamHI and XhoI restriction sites. GFP-Sar1 and DsRed-Sar1H79G were generated in pEGFP-C1 and pDsRed-Monomer-C1 vectors, respectively, by PCR to amplify Sar1 and Sar1H79G using primers which were then cloned at XhoI and KpnI sites. To generate Myc-Sar1, Sar1 was amplified by PCR and cloned into the pCMV-Myc vector at EcoRI and KpnI sites. To generate DsRed-tagged Sec24D, Sec24D was amplified by PCR using primers and cloned into pDsRed-Monomer-C1 vectors at XhoI and KpnI sites. All constructs used in the present study were verified by nucleotide sequence analysis.

### Transient transfection

Transient transfection of cells was carried out by using linear polyethyleneimine (PEI, MW 25,000). For each transfection of cells cultured on 12-well plates, 500 ng of plasmids were diluted into 21  $\mu$ L of NaCl (0.15 M). In another tube, 4  $\mu$ L of PEI (7.5 mM) was diluted with 17  $\mu$ L of NaCl. After 5 min, the two solutions were combined and incubated for additional 15 min. The mixture was added to each well containing 1 mL of DMEM plus FBS and the medium was changed after 6 h.

### RUSH assays

RUSH assays were essentially carried out as described.<sup>27,62</sup> To study the ERES, cells were seeded on 12-well plates with coverslips overnight and transfected with 500 ng of RUSH plasmids with or without co-transfection with Sec24D or Sar1H79G (500 ng) for 20 h. The cells were then fixed with 4% paraformaldehyde and 4% sucrose in phosphate-buffered saline (PBS) for 15 min. The numbers of puncta or the ERES were quantified by using NIH ImageJ and the co-localization of cargoes with Sec24D at the ERES was determined by Pearson's coefficient using the ImageJ JaCoP plugin.

To study cargo transport from the ER to the Golgi in fixed cells, cells were transfected with RUSH plasmids with or without Sar1H79G as above. The cells were then incubated with biotin at a final concentration of 40  $\mu$ M for different time periods as indicated in each figure before fixation. To study the co-localization of AT2R with different Golgi markers after biotin induction, the cells were transfected with RUSH plasmids expressing mCherry-AT2R together with p58-YFP (ER-Golgi intermediate compartment marker), venus-giantin (*cis*- and *medial*-Golgi marker),  $\beta$ 1,4-galactosyltransferase 1 (GalT)-YFP or pmTurquoise2-GalT (*trans*-Golgi and *trans*-Golgi network markers) for 20 h and then incubated with biotin for 30 min (Figure S2). For live cell RUSH assays, HeLa cells grown on 35 mm Petri dishes with glass bottom were transfected with 1  $\mu$ g of RUSH plasmids. After washing twice with Dulbecco's PBS (DPBS) and addition of 1 mL of DMEM (no phenol red) containing 10% FBS, 1 mL of biotin (80  $\mu$ M, dissolved in no phenol red DMEM with 10% FBS) plus CHX (800  $\mu$ g/mL) was added to induce receptor export. The Golgi expression of cargo proteins in both live and fixed cell RUSH assays was defined by the fluorescence intensity in the area containing highly concentrated receptors. The ER-Golgi transport was expressed as the ratio of the Golgi expression to the total expression as measured by using NIH ImageJ. In live cells, the Golgi/total ratio at each time point was subtracted from the ratio at time 0 and then normalized to the highest ratio which was defined as 100%.

### Fluorescence microscopy

All images were captured using LAS X software on a Leica Stellaris 5 confocal microscope equipped with an Okolab UNO stage top incubator with a 63x objective.<sup>27</sup> In live cell assays, images were captured at an interval of 10 s and the cells with low receptor expression without aggregation were chosen to be studied.

### Nano-Glo HiBiT extracellular detection assays

The cell surface expression of AT2R and its ExE-AxA mutant was quantified by using the Nano-Glo HiBiT extracellular detection system (Promega). Briefly, HEK293 cells were cultured in 6-well plates and transfected with the plasmid Str-KDEL\_SBP-HiBiT-EGFP-AT2R (500 ng/well) for 6

h. The cells were then split into 12-well plates and cultured for additional 20 h. The cells were washed twice with 1 mL of DPBS and suspended in 350  $\mu$ L of DPBS. After 100  $\mu$ L of cells were transferred into white 96-well plates and incubated with 50  $\mu$ L of LgBiT protein (1:1000 dilution) for 10 min at 37°C, 50  $\mu$ L of substrate (1:1000 dilution) were added into the plates and luminescence was measured in a Mithras LB940 photon-counting plate reader (Berthold Technologies).

### GST fusion protein pulldown assays

GST fusion protein pulldown assays were carried out using the MagneGST pulldown system (Promega) as described essentially.<sup>6,22</sup> Briefly, HEK293 cells were cultured on 10-cm dishes and transfected with 10  $\mu$ g of GFP-tagged COPII components for 24 h. After the cells were lysed, the expression of individual COPII components was estimated by immunoblotting. GST fusion proteins were incubated with the cell homogenates in a total volume of 400  $\mu$ L binding buffer containing 20 mM Tris-HCl (pH 7.4), 140 mM NaCl, 1% Nonidet P-40 and 10% glycerol overnight at 4°C. After washing 3 times with binding buffer, the bound proteins were solubilized in SDS gel loading buffer and detected by immunoblotting using GFP antibodies.

### Co-IP

Co-IP assays were carried out as described previously.<sup>6</sup> Briefly, HEK293 cells were cultured on 10-cm dishes and transfected with HA-AT2R together with GFP, GFP-Sar1 or GFP-Sec24 constructs (10  $\mu$ g each) for 24 h. The cells were harvested and lysed with 500  $\mu$ L of lysis buffer containing 50 mM Tris-HCl (pH 7.4), 150 mM NaCl, 1% Nonidet P-40, 0.5% sodium deoxycholate, 0.1% SDS and 1% protease inhibitors for 1 h. After centrifugation, the supernatants were incubated with 2  $\mu$ g of HA antibodies overnight at 4°C, followed by incubation with 30  $\mu$ L of protein G dynabeads for 1 h at 4°C. The beads were collected and washed 3 times with lysis buffer. Immunoprecipitated proteins were solubilized with SDS gel loading buffer and detected by immunoblotting using antibodies against HA or GFP.

### QUANTIFICATION AND STATISTICAL ANALYSIS

Details regarding the quantification of receptor expression, the ERES number and co-localization of cargo proteins with Sec24D in cells are provided in the [method details](#) section. All data were calculated and presented as mean  $\pm$  SD. Statistical analysis was performed using one-way ANOVA test. Significance levels are \* $p < 0.05$ , \*\* $p < 0.01$  and \*\*\* $p < 0.001$ .